A Walking Controller for a Powered Ankle Prosthesis

Amanda H. Shultz, Jason E. Mitchell, Don Truex, Brian E. Lawson, Elissa Ledoux, Michael Goldfarb[1]

Abstract— **This paper describes a walking controller implemented on a powered ankle prosthesis prototype and assessed by a below-knee amputee subject on a treadmill at three speeds. The walking controller is a finite state machine which emulates a series of passive impedance functions at the joint in order to reproduce the behavior of a healthy joint. The assessments performed demonstrate the ability of the powered prosthesis prototype and walking controller to reproduce essential biomechanical aspects (i.e. joint angle, torque, and power profiles) of the healthy joint, especially relative to a passive prosthesis.**

I. Introduction

A. Motivation

Transtibial amputees typically utilize passive dynamic elastic response (DER) foot/ankle prostheses. Such a prosthesis can only exhibit a single behavior, whereas the intact human ankle exhibits several different behaviors during walking. Such behaviors include passive (e.g. stiffness and/or damping) as well as active behaviors (e.g. powered push-off), each of which may vary with walking speed. Thus, a prosthesis with a single dynamic behavior (e.g. a passive DER ankle/foot prosthesis) is by nature incapable of fully reproducing the function of the intact human ankle during walking. Furthermore, the intact human ankle joint generates net positive power during both gait initiation [1] and steady-state walking, particularly self-selected medium to fast speeds [2]. Consequently, persons with below knee amputations walking on passive prostheses have been shown to require up to 20% more oxygen than healthy individuals [3]. Additionally, their walking speed has been shown to be significantly reduced [4], between 10% and 22% [5, 6].

B. Prior Work

Advances in battery, microprocessor and motor technologies have made possible the emergence of powered prostheses capable of delivering biomechanically significant levels of power during walking. A number of control strategies for walking have emerged in conjunction with these prosthetic ankle designs, several of which are reviewed in [7]. Among these strategies is a method that uses shank (tibia) angle and angular velocity to find a continuous relationship between percent of stride, stride length, and ankle angle; a variation of this method modulates the ankle period and amplitude based on stride time of the previous gait cycle [8]. Another strategy incorporates a two-state model, one for swing and the other for stance, in which the swing phase employs position control, and the stance phase incorporates a Hill-type muscle model which reacts with a force in proportion to position and speed [9]. Au et al. [10] describe a neural network approach as well as a neuromuscular model approach which utilize electromyogram (EMG) signal inputs from the amputee's residual limb to set the ankle angle. Finally, Au et al. present a control strategy in which the phases of gait are decomposed into four parts, and a finite state controller utilizes combinations of linear and nonlinear springs, a torque source, and position control for the various phases [11]. An extension of this method implements one finite state controller for level ground walking and one for stair climbing, using EMG signals from the user to switch between controllers [12].

This paper presents a finite-state impedance-based walking controller for level walking at multiple cadences. The efficacy of the controller is evaluated on a powered ankle prosthesis prototype with a single transtibial amputee subject. The biomechanical characteristics of the ankle were measured during walking at multiple cadences and compared to the corresponding characteristics of the healthy joint.

II. Prosthesis Design

A. Mechanical Design

The Vanderbilt Powered Ankle Prosthesis prototype, shown in Fig. 1, has a range of motion of 45 degrees of plantarflexion and 20 degrees of dorsiflexion. The prosthesis mass, including the battery and electronics, is 2.29 kg. The prosthesis incorporates a Maxon EC60 14-pole brushless motor, which in conjunction with a 116:1 transmission ratio can generate a peak ankle joint torque of approximately 110 Nm. The ankle-foot complex additionally incorporates a parallel spring which engages at a predetermined ankle angle and supplements the motor output with additional plantarflexive torque. For the prototype used in this work, the parallel spring stiffness was 4.2 Nm/deg, and the engagement angle 1.6 deg (dorsiflexion). A custom embedded system incorporates a 32-bit microcontroller which executes control code, a custom brushless motor servo-amplifier, ankle joint angle and angular velocity measurement, and a 6-axis inertial measurement unit (IMU). The prosthesis is powered by an on-board lithium-polymer battery and attaches to a user's socket via a standard pyramid connector.

B. Impedance-Based Control Design

The control system for the powered prosthesis is structured in two levels, the lower of which controls torque at the ankle joint, providing emulation of a desired impedance.

*This work was funded in part by NIH grant R01HD075493.

[1]A. H. Shultz, J. E. Mitchell, D. Truex, B. E. Lawson, E. Ledoux and M. Goldfarb are with the Department of Mechanical Engineering, Vanderbilt University, Nashville, TN 37235 USA. (corresponding author A. H. Shultz: e-mail: amanda.shultz@vanderbilt.edu, {jason.mitchell, don.truex, brian.e.lawson, elissa.d.ledoux, michael.goldfarb} @vanderbilt.edu)

978-1-4244-7929-0/14/$26.00

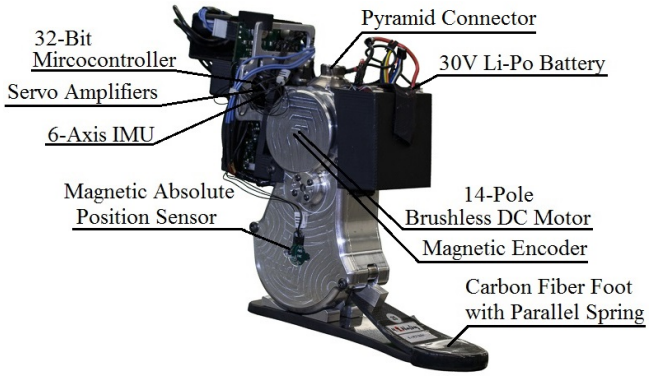

Fig. 1. Powered prosthesis prototype.

The torque reference is generated by the top level controller, which is implemented as a finite-state machine where each state is defined by passive joint impedance characteristics, modified slightly from that developed by Sup et al. [13]. Specifically, the required joint torque in each state is determined according to the following model

$$\tau = k_i(\theta - \theta_{ei}) + k_{5,i}(\theta - \theta_{ei})^5 + b_i\dot{\theta} \qquad (1)$$

where k_i, $k_{5,i}$, b_i, and θ_{ei} denote linear stiffness, nonlinear stiffness, damping coefficient, and equilibrium angle, respectively, for the i^{th} state during a gait cycle. Note that $k_{5,i}$ is nonzero only during the middle stance phase of the walking controller, where it acts as a stiffening spring term to increase ankle support as the user's center of mass (CoM) passes over the ankle joint. The anatomical ankle has been characterized as a nonlinear, stiffening spring during the phase of gait corresponding to middle stance [14]. A fifth order term was implemented as an approximation of the relationship between ankle angle and torque for healthy subjects from [15] during this phase of gait.

There are several notable differences from the control strategies previously implemented for level ground walking in powered ankle prostheses. This controller does not employ EMG signals or associated electrodes and instrumentation. Additionally, the controller does not utilize high gain position control (i.e., does not enforce a trajectory), facilitating more natural interaction between the user, the device, and the environment. Further, this device does not utilize a sensor which directly measures ground contact or load but instead infers such conditions based upon other sensor information, allowing minimization of both the quantity of sensors and device build height without jeopardizing functionality.

C. Walking Controller

The ankle behavior is segmented into four basic functions within one cycle of walking gait: damping during late swing and heel strike, (stiffening) spring-like support during middle stance, power delivery during push-off, and finally a return to a neutral ankle angle during swing. This control structure is presented in schematic form in the state chart shown in Fig. 2. Since this device does not utilize a load cell, heel strike is detected by a negative (plantarflexive) ankle angular velocity during late swing/early stance (mode 3) that occurs when

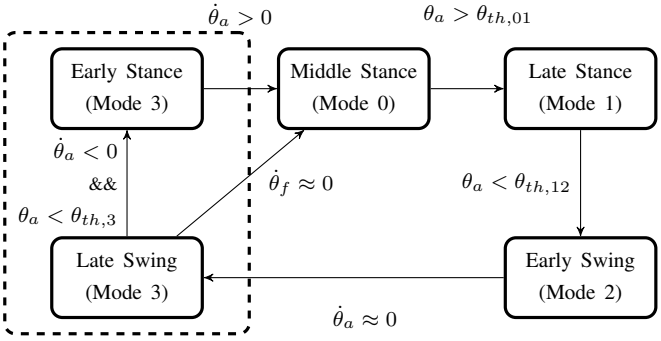

Fig. 2. The finite state machine executed by the prosthesis for walking. θ_a is the ankle angle, which is compared to predetermined thresholds $\theta_{th,01}$, $\theta_{th,12}$, and $\theta_{th,3}$, respectively. $\dot{\theta}_a$ is the angular velocity of the ankle, and $\dot{\theta}_f$ is the angular velocity of the foot with respect to the ground.

the ankle angular position is near or greater than (i.e., more dorsiflexed than) the equilibrium position for that mode.

During the early stance phase of gait (mode 3), the joint behaves chiefly as a damper, plantarflexing upon heel contact to provide shock absorption. Middle stance (mode 0) may be initiated either by heel strike detection followed by ankle dorsiflexion, or by foot flat detection (foot angular velocity approximately zero). The powered prosthesis emulates a nonlinear, stiffening spring during middle stance. Late stance (mode 1) is initiated by dorsiflexing the ankle past a predetermined angle. The physical behavior in late stance mimics push-off in healthy walking by emulating a stiffness with a virtual equilibrium point in a plantarflexed position. At this transition, the rate of change of the torque reference is limited in order to ensure there is no discontinuity in the torque reference such that it comfortable to the user. Once push-off has been completed (the ankle reaches a predetermined position threshold), the controller enters early swing (mode 2), during which the ankle returns to a slightly dorsiflexed equilibrium position for toe clearance. Late swing (mode 3) begins once the ankle has reached an equilibrium (i.e. the ankle angular velocity is essentially zero). In this mode, the controller emulates a light spring at a neutral equilibrium point and relatively high damping in preparation for heel strike.

Note that late swing and early stance are represented by two states in the state chart in Fig. 2. The behaviors of the ankle during these two phases of gait are similar and thus can be represented as a single combined mode in the controller. Notice also that, as previously mentioned, the heel strike condition in the state chart (Fig. 2) is not necessary to enter middle stance (i.e., heel strike detection is implemented primarily for the purpose of gait analysis).

III. Evaluation

A. Evaluation Metrics

The goal of this work is to assess the ability of the walking controller, as implemented on the powered prosthesis prototype described previously, to substantially reproduce biomechanical function of the healthy limb level ground walking at multiple cadences. The kinematics and kinetics of a below-

knee amputee are assessed during level walking at three speeds. Specifically, the data from walking experiments with the powered prosthesis experiments are compared to data published regarding healthy subjects and, for kinematics, data collected for the same experiment with the subject's passive prosthesis.

B. Experimental Tuning

The walking controller impedance parameters and transition conditions were determined experimentally in overground walking during a series of training trials, and subsequently on a treadmill. The controller parameters were iteratively tuned based on a combination of quantitative (ankle joint kinematic and kinetic data) and qualitative (user feedback, external observation) information, in order to provide appropriate kinematics and kinetics as well as reliable and natural gait mode transitions. This tuning process is similar to the approach implemented by a prosthetist as he or she selects passive components with appropriate stiffnesses according to the quality of gait demonstrated by the subject. A distinct set of parameters was found for each walking cadence (slow, normal, and fast), where the parameters which varied with cadence were chiefly related to the timing and strength of push-off as well as the middle stance stiffening spring component.

C. Data Collection

The subject on whom this system was evaluated is a below-knee amputee, male, age 44, with a body mass of 85.7 kg (189 lb). The subjects's passive prosthesis is an Össur Vari-Flex XC carbon fiber foot. For the assessment, the amputee subject walked with the powered prosthesis prototype on a treadmill at 0.98, 1.13, and 1.35 m/s for slow, self-selected, and fast cadence trials, respectively. These treadmill speeds were chosen based on the amputee subject's preference. Data were recorded for approximately 90 seconds of continuous, steady-state walking, for each speed, from which 20 strides were selected each and used for analysis. The same protocol was performed with the subject's passive prosthesis at the same treadmill speeds. Approval to perform these assessments was granted by the Vanderbilt Institutional Review Board, and informed consent was obtained for the subject prior to the assessments. The subject additionally gave verbal permission for the publication of photographs and video.

Ankle angle data for the powered prosthesis trials were collected via signals recorded on the prosthesis, while corresponding data for the passive prosthesis were collected via motion capture. Motion capture was performed using a twelve OptiTrack S250e infrared camera system (NaturalPoint, Inc.) to track a full skeletal marker set (similar to the Helen Hayes marker set) consisting of thirty-four reflective markers. Motion capture data were sampled at 120 Hz using ARENA software (NaturalPoint, Inc.) and subsequently exported to and processed in MATLAB in order to extract lower limb sagittal joint angles.

The periodic data were parsed into single strides and normalized to a time base of 100%. For the powered prosthesis, heel strike was determined as the point during mode 3 when the ankle angular velocity becomes substantially nonzero. Prosthesis data were processed to provide joint angles and angular velocities as well as output torque and power. The joint torque experienced by the user (output torque) was calculated using a model of the known or estimated passive characteristics of the motor, transmission, and parallel spring (i.e. inertia, friction, and stiffness); this torque was then multiplied by velocity in order to calculate power.

The passive prosthesis ankle angle motion capture data were parsed into strides based on kinematic data in a manner similar to that presented in [16, 17]. A sharp inflection of the ankle angle was used to determine heel strike in lieu of the minimum position of the heel marker used in [16].

D. Results and Discussion

Figure 3 contains kinematic and kinetic data corresponding to published healthy subject data from [15], the amputee subject walking with the powered prosthesis, and (for kinematics) the amputee subject walking with his passive prosthesis, at each of the three speeds evaluated in this work. In each plot, data characterizing plus and minus one standard deviation around the corresponding mean are shaded in gray, providing a standard for comparison which incorporates inter-subject gait variability for healthy individuals. The blue (dark) line is mean powered prosthesis data, and the red (light) line, shown in ankle angle plots only, represents mean passive prosthesis data. Note that the three treadmill speeds used in the previously described experiments corresponded to respective cadences of 91, 101, and 112 steps/min with the powered prosthesis, and 93, 104, and 110 steps/min, respectively, for the passive prosthesis. Note also that the corresponding healthy subject data shown in the plots corresponds to average cadences of 85, 105, and 125 steps/min, respectively.

The top row of Fig. 3 shows the ankle angle versus stride for the powered prosthesis, passive prosthesis, and healthy norm, for the three respective walking speeds. Note that the powered prosthesis falls largely within the healthy data band for all three speeds. Regarding the passive prosthesis, no powered push-off can be achieved, resulting in the absence of a plantarflexive peak in late stance/early swing. Additionally, notice that for all three cadences the peak dorsiflexion in stance occurred at least 10% later in the stride than for the powered prosthesis.

The middle row of Fig. 3 shows the sagittal plane ankle torque for the powered prosthesis, relative to the healthy norm. The joint torque profiles for the powered are strongly representative of healthy data, but with slightly lower magnitude. The bottom row of Fig. 3 shows the sagittal plane ankle joint power. Note that in fast walking, the power pulse observed in the powered prosthesis leads that of healthy fast walking. Due to the aforementioned output power limitations in the powered prosthesis, the authors chose to initiate power delivery slightly earlier than what is observed in healthy data

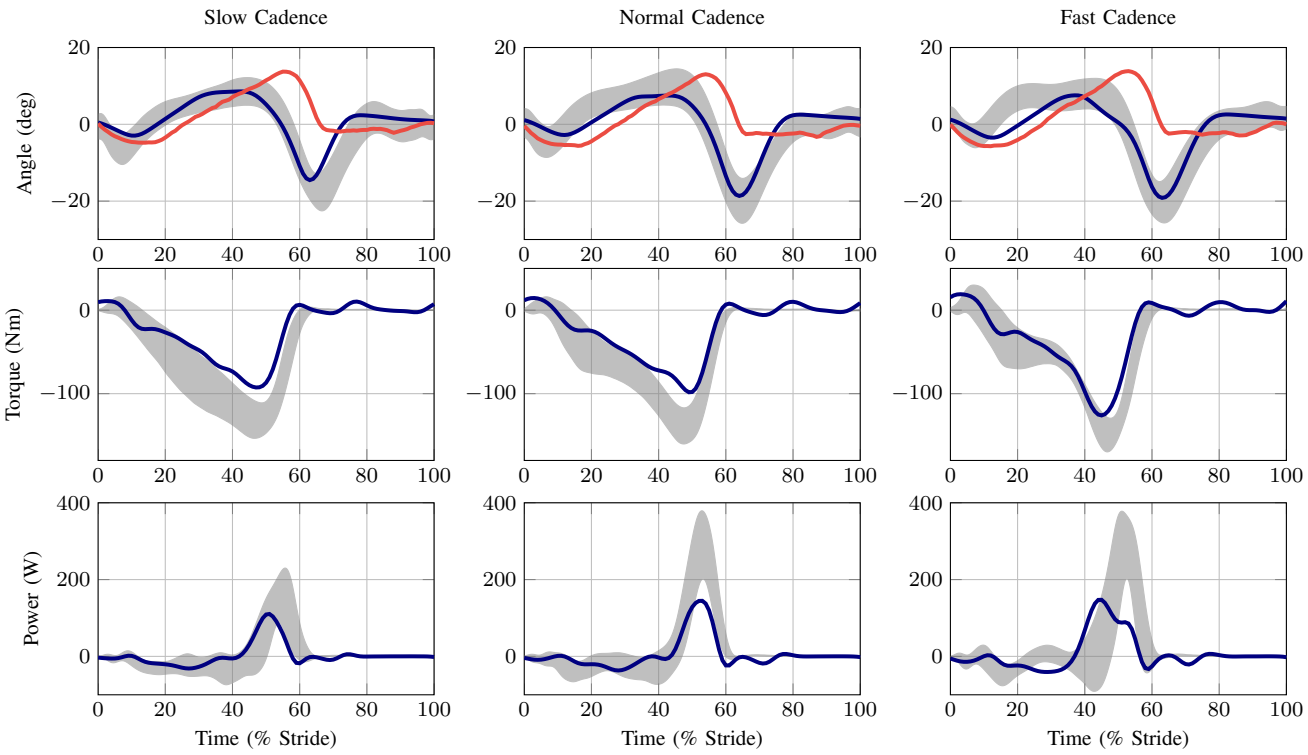

Fig. 3. Kinematics and kinetics for slow, normal, and fast cadences. Healthy subject data ± 1 standard deviation are shaded in gray, powered prosthesis data are shown by blue (dark) lines, and passive prosthesis data are shown by red (light) lines.

in order to increase power delivery. Note that, while power data are not available for the passive prosthesis, by nature it cannot deliver net positive power–and will actually dissipate net power–over a stride.

IV. Conclusion

The authors describe in this work a powered ankle prosthesis prototype and walking controller, and a corresponding assessment of these on a transtibial amputee subject at three speeds. The assessments performed demonstrate the ability of the powered prosthesis prototype and walking controller to reproduce, for a below-knee amputee subject, the essential biomechanical aspects of the healthy joint. Specifically, the system was shown to provide joint angle, torque, and power profiles representative of the healthy joint behavior, particularly relative to a passive prosthesis.

References

[1] A. H. Hansen, S. C. Miff, D. S. Childress, S. A. Gard, and M. R. Meier. Net external energy of the biologic and prosthetic ankle during gait initiation. *Gait Posture*, 31(1):13 – 17, 2010.

[2] A. H. Hansen, D. S. Childress, S. C. Miff, S. A. Gard, and K. P. Mesplay. The human ankle during walking: implications for design of biomimetic ankle prostheses. *J Biomech*, 37(10):1467 – 1474, 2004.

[3] N. H. Molen. Energy/speed relation of below-knee amputees walking on a motor-driven treadmill. *Internationale Zeitschrift fr angewandte Physiologie einschlielich Arbeitsphysiologie*, 31(3):173–185, 1973.

[4] L. Torburn, C. M. Powers, R. Guiterrez, and J. Perry. Energy expenditure during ambulation in dysvascular and traumatic below-knee amputees: a comparison of five prosthetic feet. *J Rehabil Res Dev*, 32(2):111–119, 1995.

[5] L. Torburn, J. Perry, E. Ayyappa, and S. L. Shanfield. Below-knee amputee gait with dynamic elastic response prosthetic feet: a pilot study. *J Rehabil Res Dev*, 27(4):369–384, 1990.

[6] R. D. Snyder, C. M. Powers, C. Fountain, and J. Perry. The effect of five prosthetic feet on the gait and loading of the sound limb in dysvascular below-knee amputees. *J Rehabil Res Dev*, 32(4):309–315, 1995.

[7] R. Jimnez-Fabin and O. Verlinden. Review of control algorithms for robotic ankle systems in lower-limb orthoses, prostheses, and exoskeletons. *Medical Engineering & Physics*, 34(4):397 – 408, 2012.

[8] M. A. Holgate, A. W. Bohler, and T. G. Sugar. Control algorithms for ankle robots: A reflection on the state-of-the-art and presentation of two novel algorithms. In *In Proc. IEEE/RAS-EMBS Int. Conf. Biomed. Robot. Biomechatron.*, pages 97–102, 2008.

[9] M. F. Eilenberg, H. Geyer, and H. Herr. Control of a powered ankle-foot prosthesis based on a neuromuscular model. *IEEE Trans. Neural Syst. Rehabil. Eng.*, 18(2):164–173, 2010.

[10] S.K. Au, P. Bonato, and H. Herr. An emg-position controlled system for an active ankle-foot prosthesis: an initial experimental study. In *In Proc. IEEE Int. Conf. on Rehabilitation Robotics*, pages 375–379, 2005.

[11] S.K. Au, P. Dilworth, and H. Herr. An ankle-foot emulation system for the study of human walking biomechanics. In *In Proc. IEEE Int. Conf. on Robotics and Automation*, pages 2939–2945, 2006.

[12] S. Au, M. Berniker, and H. Herr. Powered ankle-foot prosthesis to assist level-ground and stair-descent gaits. *Neural Networks*, 21(4):654 – 666, 2008. Robotics and Neuroscience.

[13] F. Sup, A. Bohara, and M. Goldfarb. Design and control of a powered knee and ankle prosthesis. In *In Proc. IEEE Int. Conf. on Robotics and Automation*, pages 4134–4139.

[14] M.L. Palmer. Sagittal plane characterization of normal human ankle function across a range of walking gait speeds. Master's thesis, Massachusetts Institute of Technology, 2002.

[15] D. A. Winter. *The Biomechanics and Motor Control of Human Gait: Normal, Elderly and Pathological*. University of Waterloo Press, Waterloo, Ontario, Canada, 2nd edition, 1991.

[16] I. P. I. Pappas, M. R. Popovic, T. Keller, V. Dietz, and M. Morari. A reliable gait phase detection system. *IEEE Trans. Neural Syst. Rehabil. Eng.*, 9(2):113–125, 2001.

[17] J. K. De Witt. Determination of toe-off event time during treadmill locomotion using kinematic data. *J Biomech*, 43(15):3067 – 3069, 2010.